Atmos. Chem. Phys. Discuss., 7, 6767–6801, 2007
www.atmos-chem-phys-discuss.net/7/6767/2007/

Atmospheric Chemistry and Physics Discussions

Lightning and convection parameterisations – uncertainties in global modelling

H. Tost, P. Jöckel, and J. Lelieveld

Atmospheric Chemistry Department, Max-Planck Institute for Chemistry, P.O. Box 3060, 55020 Mainz, Germany

Received: 13 April 2007 – Accepted: 4 May 2007 – Published: 21 May 2007

Correspondence to: H. Tost (tost@mpch-mainz.mpg.de)

Abstract

The simulation of convection, lightning and subsequent NO_x emissions with global atmospheric chemistry models is associated with large uncertainties since these processes are heavily parameterised. Each parameterisation by itself has deficiencies while the combination substantially increases the uncertainties from the individual parameterisations. In this study several combinations of state-of-the-art convection and lightning parameterisations are used in model simulations with the global atmospheric chemistry model ECHAM5/MESSy and are evaluated against lightning observations. A wide range in the spatial and temporal variability of the simulated flash densities is found, attributed to both types of parameterisations. Some combinations perform well, whereas others are hardly applicable. In addition to resolution dependent rescaling parameters, each combination of lightning and convection schemes requires individual scaling to reproduce the observed flash frequencies. The resulting NO_x profiles are inter-compared, but definite conclusions about the most realistic profiles can currently not be provided.

1 Introduction

Lightning represents one of the most energetic phenomena in the Earth's atmosphere. In the troposphere flashes are the only natural process that can break up the highly stable triple bonds of molecular nitrogen, transforming N_2 into reactive nitrogen species which strongly influence the chemistry of the upper troposphere (e.g. Labrador et al., 2005; Schumann and Huntrieser, 2007, and references therein). Therefore, an accurate representation of lightning in global models of the atmosphere is crucial. Additionally, lightning represents an important factor in the ignition of wild fires (e.g. Jacobson, 2002).

In contrast to small scale process models (e.g. Barthe et al., 2005) atmospheric chemistry general circulation models (AC-GCMs) generally do not represent the global

electrical circuit, e.g. the electrical field and the detailed processes involved in cloud electrification and discharges. Instead the lightning and the subsequent NO_x formation are determined with the help of (semi-)empirical parameterisations. Since it is difficult to measure such emissions in situ or by remote sensing, there is a high uncertainty in the total amount of NO_x produced by lightning, i.e. ranging from 2 to 12 Tg N/yr (e.g. Beirle et al., 2004; Schumann and Huntrieser, 2007). The occurrence of flashes on the other hand can be observed from satellites, e.g. the LIS/OTD missions (Christian et al., 1999, 2003; Thomas et al., 2000), and an extensive climatology over the last decade has been established and used for comparisons with parameterisations. Even if the occurrence of flashes could be predicted accurately by the model, uncertainties in the NO_x emissions remain, since the amount of NO_x produced per flash is not a constant. It varies with flash strength, extension, type, branching, and additional aspects. The amount of NO_x per flash in a "typical thunderstorm" varies by more than an order of magnitude ($(2-40)\times10^{25}$ NO molecules per flash) (Schumann and Huntrieser, 2007). Nevertheless, the accurate prediction of flash occurrence is a prerequisite to estimate lightning produced NO_x emissions in the upper troposphere. A problem with most parameterisations (some will be described in detail below) is that they are mainly derived empirically from correlations between other observable quantities. However, their applicability to the global scale and extended time periods of several years is limited since the heterogeneity of phenomena can only be represented approximately. Nevertheless, these parameterisations are used in global AC-GCMs since simulated lightning events should coincide with the occurrence of convection and the assimilation of observed flashes at every model timestep is computationally not feasible and not necessarily consistent with the occurrence of convection in the model. Furthermore, for calculation of future scenarios such techniques are not applicable and the lightning has to be parameterised. Petersen and Rutledge (1998) found a relationship between convective precipitation and lighting with the goal to estimate the rain rate from observed flashes. Even though a precipitation estimate can be made from lightning events, this study concludes that this is only valid for long-term averages, and not

to individual precipitation and related lightning events (Petersen and Rutledge, 1998). Further studies of Petersen et al. (2005) combining satellite observations of precipitation ice water content and flashes show that the correlation of these two parameters can be applied globally, almost for individual events, but unfortunately convection parameterisations include too strongly simplified cloud microphysics so that the ice water content is difficult to determine accurately. Therefore, the implementation of a lightning parameterisation for GCMs based on the ice water content is not straight-forward. On the other hand, the simulation of lightning based on convection parameterisations offers the possibility to investigate how realistic these schemes describe the processes. In a previous study (Tost et al., 2006) we analysed convection on a global scale with respect to temperature and the hydrological cycle using several convection parameterisations, but did not discuss the convective dynamics, e.g. the convective mass fluxes. With the help of the updraft based lightning schemes (details below), the updraft strength can be correlated to the observable quantity of flashes.

The next section introduces the model and the parameterisations used, Sect. 3 the simulation setup. Section 4 presents the analysed results, and the conclusions are given in Sect. 5.

2 Model description

In this study the AC-GCM ECHAM5/MESSy (E5/M1) (Jöckel et al., 2006) has been applied. It is based on the general circulation model ECHAM5 (Roeckner et al., 2006) (version 5.3) and the Modular Earth Submodel System (Jöckel et al., 2005) (version 1.3).

Most of the meteorological processes are calculated by ECHAM5 based on a spectral representation of the prognostic variables vorticity, divergence, temperature, and the logarithm of the surface pressure, as well as grid point representations of specific humidity, cloud water, and cloud ice. In the vertical a hybrid pressure coordinate system is applied. The processes of radiation and cloud microphysics are parameterised,

as described in the ECHAM5 documentation (Roeckner et al., 2003, 2004).

Additionally, the MESSy infrastructure and some of the submodels, i.e. an extended convection submodel (Tost et al., 2006) containing additional parameterisations, an extended lightning NO_x emission submodel (LNOX) and the diagnostic tropopause and planetary boundary layer height submodel (TROPOP) have been used.

2.1 Convection parameterisations

The convection parameterisations included in the CONVECT submodel are:

- The Tiedtke (1989) scheme with modifications by Nordeng (1994) (further denoted as T1). This scheme is used as the default convection parameterisation.
- The convection parameterisation of the operational ECMWF model (IFS cycle 29r1b, further denoted as EC) (Bechtold et al., 2004, and references therein), which is a further development of the Tiedtke (1989) scheme;
- The Zhang-McFarlane-Hack scheme (Zhang and McFarlane, 1995; Hack, 1994) (ZH) as applied in the MATCH model (Rasch et al., 1997; Lawrence et al., 1999) and a version with an extended evaporation scheme (Wilcox, 2003), denoted as ZHW;
- The scheme of Bechtold et al. (2001), further denoted as B1.

For a more detailed comparison of these schemes, their detailed configurations and extensions, and their influence on the hydrological cycle we refer to Tost et al. (2006) and Tost (2006).

2.2 Lightning parameterisations

The LNOX submodel applied in this study encompasses the widely used lightning NO_x parameterisation by Price and Rind (1992) with further updates (Price and Rind, 1993,

1994; Price et al., 1997a,b) based on the correlation between the convective cloud top height and the occurrence of flashes derived from regional observations (**P_cth**):

$$F_c = 3.44 \times 10^{-5} \cdot H^{4.90} \qquad (1)$$
$$F_o = 6.40 \times 10^{-4} \cdot H^{1.73},$$

with F_c representing the continental and F_o the oceanic flash frequencies and H the convective cloud top height in kilometres above ground. For each grid box the total flash frequency is determined by weighting with the fractional land-sea mask. In addition, the parameterisation by Grewe et al. (2001) is included, linking updraft velocity as a measure of convective strength and associated cloud electrification with the flash frequency (**G_updr**):

$$F = 1.54 \times 10^{-5} \cdot (w \cdot d^{0.5})^{4.9}, \quad \text{with :} \qquad (2)$$
$$d = \sum_{i=\text{cloud bottom}}^{\text{cloud top}} h_i$$
$$w = \sum_{i=\text{cloud bottom}}^{\text{cloud top}} M_i/\rho_i(h_i/d),$$

with F the flash frequency, w the updraft velocity, h_i the grid box height, d the cloud thickness, M_i the updraft mass flux and ρ_i the air density. Note that there is no differentiation between land and sea, assuming that the weaker intensity of convection (and consequently less intense cloud electrification) over the ocean is represented adequately by the convection parameterisation. Allen and Pickering (2002) propose two additional polynomial parameterisations for lightning occurrence, one also based on the updraft strength at a specific altitude (**A_updr**):

$$F_{cg} = a + b \cdot M + c \cdot M^2 + d \cdot M^3 + e \cdot M^4, \qquad (3)$$

and another on the amount of convective precipitation at the surface (**A_prec**):

$$F_{cg} = a_i + b_i \cdot P + c_i \cdot P^2 + d_i \cdot P^3 + e_i \cdot P^4 \qquad (4)$$

with M the updraft mass flux at 0.44 σ, and P the convective precipitation at the surface (only for precipitation stronger than 7 mm/day). The parameters $a, b, c, d, e, a_i, b_i, c_i, d_i, e_i$ are constant, but the parameters for the precipitation based approach depend on land or ocean surface. For the total flashes (over both land and ocean) calculated with the A_prec scheme a weighting with the fractional land-sea mask has been applied (similar to the P_cth scheme). Note that these polynomial parameterisations determine the cloud-to-ground flashes (F_{cg}) only, whereas the first two approaches give the total flash frequency (cloud-to-ground and in-cloud). Nevertheless, with the help of the relationship between cloud-to-ground and total flash frequency by Price and Rind (1993), for all four schemes the total amount of flashes and the fractionation into cloud-to-ground and in-cloud can be determined.

3 Simulation setup

A set of five simulations has been performed in a horizontal resolution of T42 (≈2.8°×2.8° of the corresponding quadratic Gaussian grid) and 31 layers in the vertical direction (the midpoint of the uppermost layer is at 10 hPa). In each simulation all four lightning parameterisations are applied simultaneously and the emitted NO_x is vertically distributed according to a parameterisation of Pickering et al. (1998). Horizontal resolution dependent scaling factors for the flash densities have been applied as proposed in the original articles describing the lightning parameterisation schemes. The individual simulation setups differ only with respect to the convection scheme selected via a namelist. Consequently, all simulations have been performed with the same executable. Because of the feedback of the convection on the atmospheric dynamics the meteorology is different for each simulation. The simulation is performed for the year 1999, with several months of model spin-up. To overcome the issues of different meteorology in the various simulations the "nudging" (Newtonian relaxation) technique (Jeuken et al., 1996; van Aalst et al., 2004; Jöckel et al., 2006) with ECMWF – operational analysis data of vorticity, divergence, temperature and surface pressure for the

year 1999 is applied. Even though the influence of the nudging is relatively small, it is sufficient to achieve similar meteorological patterns as observed in this specific year.

4 Results

Observational datasets

Observed lightning data is used from the LIS (Christian et al., 1999; Thomas et al., 2000) and OTD (Christian et al., 2003) satellite instruments[1]. In this study the gridded products of the time series for the year 1999 are applied as well as annual and daily climatologies (both at high (0.5°) and low (2.5°) resolution).

Additionally, satellite data from the Tropical Rainfall Measuring Mission (TRMM) (Kummerow et al., 2000), i.e. the 3A25 product [2], are used for the comparison of lightning data with observed convective cloud properties (convective precipitation, cloud top height). This is suitable since all satellite products are obtained from the same space platform.

4.1 Annual average lightning distributions

Figure 1 shows the annual average flash density for the year 1999 taken from the long-term time series of observed flashes from combined LIS and OTD data, i.e. the LISOTD_LRTS_V2.2 dataset. The displayed region is restricted to 60° S to 60° N because of the viewing angle of the satellite. The observed maxima occur over the continents, especially in Central Africa, with secondary maxima over South America and

[1] obtained from the Global Hydrology Resource Centre: http://thunder.msfc.nasa.gov/data/

[2] monthly mean gridded data from the precipitation radar, a 13.8 GHz radar, one of three rain instruments carried on board the TRMM satellite, with the ability to retrieve three-dimensional precipitation characteristics

the islands of the maritime continent. Note that the colour scale of Fig. 1 is logarithmic, because of the large contrast in flash densities over the continents and the oceans.

Figure 2 shows the simulated flash densities with the different convection and lightning parameterisations. The colour scale is identical to that of Fig. 1. However, the simulated flash frequency had to be rescaled with the average number of flashes per second over the globe (48.81 flashes/s for the year 1999, regridded on the model coordinates, from 60° S to 60° N). The scaling factors for the different model setups are listed in Table 1. This scaling, in addition to the resolution dependent rescaling mentioned above in the formulation of the lightning parameterisation, is needed for comparison and forces the results into the same range as observed.

These scaling factors differ by almost three orders of magnitude, showing the large variation of the input data from the different convection schemes for each of the lightning parameterisations. Using the convective cloud top height based parameterisation (P_cth, Eq. 1) (first column of Fig. 2) all simulations show the strong contrast between ocean and land. However, the oceanic flash densities are systematically too low by approximately a factor of 2 to 10. The maximum values occur mainly over South America whereas the high flash densities over Africa are captured only with the ZH, the ZHW and the B1 simulation (lower three panels of the first column). Except for the EC simulation the simulated lightning activity over the maritime continent is substantially overestimated. In the midlatitudes of the northern hemisphere the simulated flash density is lower than observed, most pronounced in the southern part of the USA. The updraft based lightning parameterisation of Grewe et al. (2001) (Eq. 2) (second column of Fig. 2) results in an overestimated lightning activity over the ocean compared to the observations. In combination with the T1 and EC convection schemes the simulated flash density represents the observed patterns, whereas the African maximum is not captured accurately. However, the T1/G_updr combination (second panel in the first row) yields higher values in the Southern USA, whereas in Siberia the occurrence of flashes is significantly underestimated. Even though the lightning activity over the ocean is overestimated, very high lightning activity over the continents occurs

less frequently and less localised in combination with T1 and EC. The simulations with the ZH and ZHW convection schemes are characterised by significant lightning in the midlatitude storm tracks, where a weaker land-sea contrast occurs, and stronger differences over land and sea in the tropics and subtropics. In some regions, especially over mountain slopes (Himalaya, Andes) very high flash densities are calculated. The latter effect results partly from the convection scheme which computes high convective mass fluxes at these locations. The combination of the B1 convection with the G_updr lightning results in very spotty flash occurrences. The observed flash distribution is not well reproduced. This is obviously caused by the strong exponential dependency of the lightning frequency on the vertical velocity, because applying the same mass fluxes with the A_updr scheme, these spikes do not occur (compare third panel of the last row). Additionally, the possible occurrence of unrealistically strong shallow convection can affect the mean vertical velocity within the cloud, whereas for the A_updr scheme the updraft strength at 0.44 σ, i.e. approx. 500 hPa is used.

Using the polynomial fit of updraft for the flash frequency (A_updr, Eq. 3), the lightning over the ocean is even more strongly overestimated as with G_updr, and the continental maxima are substantially underestimated when it is applied in combination with the T1 and EC convection (upper two panels of the third row of Fig. 2). Furthermore, the extratropical continental lightning density is too low. In combination with the ZH and ZHW convection a similar distribution as with the G_updr occurs with the maxima in the same locations, not capturing the observed ones, especially over the continents. This cannot be attributed to shallow convection, but rather to the total number of convective events. Moreover, the updrafts in the middle and upper troposphere are substantially weaker compared to the other schemes, which results in the high rescaling factors for these combinations in Table 1, but they are more widely distributed over large regions of the globe. The strong activity in the storm tracks results from the setup of the convection parameterisation: in the midlatitudes the adjustment scheme following the approach of Hack (1994) instead of the deep convection of Zhang and McFarlane (1995) is activated. This results in an overestimation of the convection and consequently an

underestimation of large scale condensation processes (compare Tost et al., 2006). Additionally, this might be partly caused by the nudging, since the boundary layer stability is directly involved in the triggering of the convection algorithm. The nudging causes slightly enhanced stability, since for the nudged temperature profile, convection and boundary layer parameterisations have been applied at data generation. This can cause a decrease of the convective activity. A simulation without nudging showed substantially stronger mass fluxes in the middle and upper troposphere (Tost, 2006). In contrast, the combination with the B1 convection results in a much smoother lightning distribution. The absolute maximum in Central Africa is shifted too far northward, and the flash density is overestimated over the tropical oceans, while localised events such as with G_updr do not occur (as mentioned above) if the mass flux at about 500 hPa is used to determine the number of flashes. The precipitation based approach of Allen and Pickering (2002) (Eq. 4) combined with the T1 convection (upper panel in the last row) does not reproduce the observed land-sea contrasts. The maximum in Central Africa is underestimated as well as the flash densities in Europe, North America and Siberia. On the other hand, the values in the ITCZ over all oceans, the warm pool region and the SPCZ are overestimated by a factor of 5 to 10. Some of these high values over the ocean do not occur when used with the EC convection scheme, but still the oceanic flash density is overestimated compared to the observations. This results from the lower total amount of convective precipitation than with T1 produced in this regions (compare Tost et al., 2006). However, in South America, higher values than observed are simulated, and the maximum over Central Africa is poorly reproduced. Similarly to T1, the occurrence of lightning in the continental midlatitudes of the Northern hemisphere is underestimated, since the contribution of convective precipitation during frontal passages may be too low, i.e. the nimbostratus clouds associated with midlatitude precipitation are not formed by the convection but by the large-scale condensation scheme. The ZH and ZHW convection schemes, which yield a strong difference between precipitation over land and sea (Tost et al., 2006), capture the distribution slightly better, but strongly overestimate the flash frequency over the tropical

continents (especially ZH). On the other hand, in the midlatitudes continental lightning is underestimated, though less compared with the other convection schemes. The combination of B1 and A_prec results in a more realistic distribution of the annual average flash density. Even though the maximum over Central Africa is underestimated, and the values over the tropical oceans overestimated, the general patterns are captured quite well, and especially the extreme values over specific locations do not occur.

A statistical comparison of the observed and simulated annual average flash densities is shown with the help of a Taylor diagram in Fig. 3 (Taylor, 2001). In combination with the P_cth scheme the overall performance of all convection schemes is very similar (all "X"s are closely together, the green and the red ones mainly overlay). This indicates a very robust behaviour of this approach. However, even though the cloud top height differs and depends on the scheme, the average distribution agrees well in all simulations. The correlation ($R \approx 0.75$ to 0.8) is highest for these combinations, but the spatial variation is slightly overestimated ($\sigma^\star \approx 1.2$ to 1.4 with $\sigma^\star = \sigma_{\mathrm{sim}}/\sigma_{\mathrm{obs}}$). The T1/G_updr combination achieves a similar correlation, but a lower $\sigma^\star$ indicating a better performance in this simulation setup. However, it must be considered that this approach is not working well with the other convection parameterisations since it is highly dependent on the vertical updraft velocity. While R is much lower for EC/G_updr, $\sigma^\star$ is close to one, whereas the symbols for ZH, ZHW and B1 are out of scale ($\sigma^\star > 2$). The polynomial fit of lightning and mass fluxes at about 500 hPa is slightly more robust, but shows a large scatter in combination with the convection parameterisations. None works as well as the P_cth approach, with respect to both correlation and spatial variation. The precipitation based approach underestimates the spatial variation for T1, EC, and B1, but overestimates it for ZH and ZHW, resulting from a worse agreement of the precipitation distributions of the latter two schemes (Tost et al., 2006). Especially the combination B1/A_prec works almost as well as T1/G_updr in capturing the observed flash density distribution.

4.2 Applicability of lightning parameterisations

To check the applicability of the lightning parameterisations monthly mean TRMM observations between 40° N and 40° S are used with the P_cth scheme as depicted in Fig. 4.

Using the cloud top based parameterisation with the observed cloud top heights (5 and 0.5 degree resolution) and applying a similar rescaling (for the high resolution data figure not shown) the maximum in Central Africa is well reproduced with respect to shape, position and strength for the low resolution data (for the high resolution data, the maximum is located too far northward), whereas in the northern part of South America lower values than observed are calculated. Additionally, the highest values for the flash occurrence over South America are shifted southward and to the Andes. In North America the highest flash density is not calculated only in the Southeast, but also more to the West. In Indonesia, flash rates similar to the observed are calculated from the observed cloud top height. The flash densities over the ocean are much smaller than over the continents, in agreement with the observed land-sea contrast. Even though high cloud top heights in the Himalaya region are observed from TRMM the resulting flash densities are relatively low due to the high surface elevation which leads to a smaller vertical extension of the cloud. The land-sea contrast and the main features of the spatial distribution can be reproduced with these calculations. However the correlation of the observed flash densities with the calculated flash densities from the observed cloud top heights is not better than for the model results, with R=0.74 for the low resolution and R=0.69 for the high resolution TRMM convective cloud top data, indicating that the monthly mean cloud top heights are probably not sufficient to reproduce the observed flash frequencies.

A similar comparison of offline calculated flash frequencies with the A_prec parameterisation is not possible since it is designed for strong individual precipitation events with a threshold value of more than 7 mm/day, which is hardly reached in the monthly averaged TRMM data. Nevertheless, the correlation between the annual average con-

vective precipitation and flash densities is determined to analyse, if the spatial distribution can be correctly reproduced as stated by Petersen and Rutledge (1998). The correlation is R=0.33 for the low resolution and R=0.32 for the high resolution annual average TRMM convective precipitation fields with the annual average observed flash densities for the year 1999. Consequently, a significant correlation, as seen in Fig. 3 for the precipitation based lightning scheme, results mainly from the suitable fit of the strong precipitation events (stronger than 7 mm/day) and only to a minor degree from the average precipitation distribution.

4.3 Annual cycle of lightning

Figure 5 depicts the annual cycle of the spatially averaged (from 60° S to 60° N) flash densities in the different simulations. As expected from Fig. 3 using the P_cth lightning parameterisation yields a similar annual cycle for all simulations (upper left panel). The black line, depicting the observed annual cycle and the grey shaded area (showing the one σ spatial variation), show a strong maximum in boreal summer. This is also captured by the simulations, but the model calculates the highest flash densities about one month earlier than observed, independent of the choice of the convection scheme. Additionally, slightly higher values than observed are simulated. Only in January, February and March, during which slightly enhanced lightning occurrence is observed, all simulations substantially overestimate the global average flash frequency (~30%). Due to the scaling this leads to slightly lower values during most of the rest of the year. The overestimation at the beginning of the year results mainly from the tropics (10° S to 10° N), since the observations show a substantially smaller maximum during the first crossing of the equator by the ITCZ in boreal spring compared to the second maximum in autumn, whereas in the simulations both crossing events result in similar lightning activity. The lightning activity during the summer periods in each hemisphere (10° to 30°) is captured in agreement with the observations. However, even if the observed TRMM cloud top height is used with the P_cth flash parameterisation, the annual cycle cannot be reproduced correctly, since double peaked maxima in May and August are

calculated with significantly lower values in July (dashed line in the upper left panel of Fig. 5). The G_updr (upper right panel of Fig. 5) scheme has much greater difficulty to reproduce the observed annual cycle of lightning activity. In combination with T1 the temporal variability of the simulated flash densities does not have shape features in common with the observations. Even though the variability ranges from 0.008 to 0.012 it does not reproduce the annual cycle. As for the P_cth scheme, the largest differences between the observed and simulated annual cycle originate from the central tropics (10° S to 10° N) showing relatively poor agreement. The changing location of the ITCZ with time cannot be detected in the lightning densities calculated with this parameterisation, largely independent of the convection scheme. T1 and EC show a smaller variability over the year compared to ZH, ZHW and B1. Especially the latter is characterised by very large temporal extremes. In combination with the poor correlation, indicated by the spatial analysis in Fig. 2, this leads to the conclusion that local extrema govern the flash densities in this simulation setup. Even though the absolute variability is much lower when the A_updr scheme is used (lower left panel of Fig. 5), the annual cycle cannot be reproduced with this parameterisation, either. T1 and EC show a similar behaviour as in the upper right panel, with hardly any annual cycle. The other three convection parameterisations are characterised by low values during the maximum of the observations (July, August, September) and higher values during the rest of the year. The reason for this can again be found in the central tropics, where the annual cycle is not captured, or is even inverse to the observations. A similar conclusion is drawn based on the lower right panel of Fig. 5, again showing large discrepancies for all convection schemes when used with the A_prec flash frequency parameterisation. As before, the major differences occur between 10° S and 10° N, the region with the strongest precipitation, and therefore (with this scheme) also lightning activity. Comparing the annual cycle of precipitation of TRMM data in this region with the simulated flash densities from the A_prec parameterisation overall agreement is found, apart from a forward shift of one month in the simulated flashes. Monthly mean precipitation data from the simulations show a very different annual cycle when T1 and

EC are used (explaining the absence of an annual cycle), whereas ZH, ZHW and B1 capture one maximum almost correctly, but all fail in accurately describing the annual precipitation cycle.

4.4 Diurnal cycle of lightning

In contrast to reproducing the annual cycle the diurnal cycle of the flash densities is captured much better by the model simulations, in general for all combinations of convection and lightning parameterisations; only ZH and ZHW perform worse in combination with the updraft based lightning parameterisations. Figure 6 depicts the diurnal cycle in UTC. Note that for the observations it is not the daily climatology for 1999, but data from several years, i.e. the "LISOTD_LRADC_V2.2" dataset. The upper left panel, showing the P_cth scheme, is able to reproduce the first flash density maximum at 14:00 UTC (related to the African lightning activity (e.g. Price and Rind, 1994)), but the second maximum which relates to the American early afternoon is generally underestimated. Since the South American flash density is simulated well or even overestimated, this must be related to the underestimation of North American lightning activity. Due to an overestimation of the maximum and the rescaling of the global flash density to the observations, the model mainly underestimates the lightning activity during the rest of the day, especially around midnight. Most of the schemes compute the diurnal cycle almost within the spatial variation of the observations being also in agreement with the results of Nickolaenko et al. (2006). The updraft base approach (G_updr) reproduces the observations well in combination with the T1 convection, especially the double peaked maxima in the afternoon and evening. With the EC convection the diurnal cycle is less pronounced. ZH, ZHW and especially B1, all shown to have problems already in our earlier analyses, also fail with respect to the diurnal cycle, showing maximum values during the night, i.e. highest lightning activity in the western part of South America (late afternoon in the Andes region, compare Fig. 2). Using the A_updr scheme, the agreement of the T1 and EC simulation with the observations is comparable to the P_cth approach. As above, the North American lightning activity (evening

hours in UTC) is underestimated. ZH and ZHW show a similar behaviour as with the G_updr parameterisation with highest values around midnight, but with two smaller maxima corresponding to the African and American lightning activity. B1 captures the diurnal cycle comparable to T1, with an overestimation of the first maximum and a forward shift of one hour, while the second maximum is not simulated. The precipitation based flash parameterisation reproduces the general features, but also fails with respect to the second evening maximum. Only with ZHW the amplitude of the diurnal cycle is underestimated. In general, the diurnal cycle represents to some degree also the spatial patterns, since the more intense continental convection occurs usually in the early afternoon. Therefore the diurnal lightning cycle is characterised by a local afternoon maximum.

4.5 NO_x emission profiles

The most important impact of lightning parameterisations in atmospheric chemistry models is on the vertical profiles of the NO_x emissions. Figure 7 depicts average NO_x emission profiles: the colours denote the convection schemes and the panels the various lightning and subsequent emission parameterisations. The upper left panel (P_cth) exhibits a similar shape for EC, ZH and ZHW after applying the flash frequency rescaling. The double peaked shape of T1 originates from the differentiation by the convection scheme between deep and midlevel convection (i.e. penetrative convection triggered above the boundary layer). Due to the formulation of the Tiedtke scheme, the second type is artificially restricted to a cloud top of 400 hPa, though globally occurs more often than deep convection. Since the vertical extension of these clouds also extends more than 3 km they are also considered for possible lightning production and cause the lower peak. Even though the EC convection is also based on the original Tiedtke scheme and offers the same types of convection, the midlevel convection cloud top is not restricted and consequently the second peak is not present. The Bechtold scheme is characterised by the emission maximum at slightly higher altitude (originating from higher cloud top levels), but of smaller magnitude. The latter effect can

result from the different freezing altitude and consequently the partitioning into cloud-to-ground and intra-cloud flashes. The application of the G_updr parameterisation results in a similar shape of the emission profiles for T1, EC, and B1, and a maximum at lower altitude with ZHW and even lower for ZH. The height of the maximum emission differs by about 150 hPa. Additionally, the overall amounts of emitted NO_x differ substantially (factor of 2), even though the total number of flashes are rescaled to the observed number. Additionally, the emissions in the mid-troposphere are substantially enhanced with ZH and ZHW.

A similar result is obtained when using A_updr with the different convection schemes: T1, EC, and B1 are similar in emission strength and the altitude of the maximum emission level, whereas for ZH and ZHW the maximum is located substantially lower, while the total amount of emitted NO_x is much larger. As with G_updr the emissions are much stronger between 400 and 700 hPa using ZH or ZHW. The precipitation based lightning scheme (A_prec, lower right panel of Fig. 7), shows approximately the same maximum emission altitude for all convection parameterisations. The total amount of emitted NO_x varies by 20%, being highest for T1 and ZH, and lowest for B1, while the general shape of the emission profiles is similar. Overall, using the different combinations of schemes results in very different distributions of NO_x from lightning, even in the average profiles. These profiles must be considered together with the spatial and temporal distribution of the lightning events to represent the instantaneous lightning NO_x emissions. The evaluation of the impacts of these emissions on atmospheric chemistry is beyond the scope of this study and will be analysed in a following publication.

4.6 Dependencies on the model resolution

Even though most of the lightning parameterisations take the dependence on the horizontal resolution into account, this is mainly done by a rescaling factor (determined from the ratio of the model grid size to a reference area) that is multiplied with the flash rate. However, for some model configurations this is probably not sufficient. Instead, a new set of parameters might be required to give a better representation of the differ-

ent convective conditions caused by the change in resolution. A sensitivity simulation using the T1 convection scheme, but a lower vertical resolution (19 Levels, but the midpoint of the uppermost layer also at 10 hPa) results in strong differences in combination with the G_updr scheme, due to differences in the convective updraft mass fluxes. For instance, the spatial distribution is captured similarly, the required rescaling factor is lower and the annual cycle for the lightning activity is represented much better in this model configuration as in the 31 layer version discussed above, being comparable to the results with the P_cth scheme. This leads to the conclusion that the vertical resolution is quite relevant for the parameterised convective dynamics and consequently that probably the parameters of the lightning scheme must be adjusted as well, depending on the vertical resolution of the model.

4.7 Potential weaknesses of the convection schemes

The analysis of the simulated lightning data in combination with the observations also indicates some weaknesses in the convection schemes:

- The convective cloud top heights differ substantially, as can be seen from the range of the rescaling factors for the P_cth lightning parameterisation as well as from the direct comparison of the cloud top heights. Furthermore, observed and simulated cloud top heights show significant differences, comparable to the study of Kurz and Grewe (2002).
  This becomes most pronounced in South America, where in contrast to the observations, the convection reaches deeper with most convection parameterisations than in Central Africa.

- The restriction of midlevel convection below 400 hPa in the T1 convection parameterisation appears to be artificial. The explicit distinction between deep convection originating close to the surface and penetrative convection starting at higher altitude is rather arbitrary, and only applied in the T1 scheme. The EC scheme, also

being developed from the original Tiedtke (1989) scheme but treating midlevel convection similar to deep convection, does not show such a clear distinction.

- Even though the convective mass fluxes agree relatively well in the zonal averages (Tost, 2006), the updraft strength of individual convective events can be too strong and / or too localised (especially with B1). On the other hand, the average vertical velocities in ZH and ZHW appear to be much lower (very high rescaling factors are required in the updraft based lightning schemes), and the convective mass fluxes in the middle and upper troposphere are lower compared to the other schemes. However, this is may be caused by the nudging.

- Oceanic convection is almost as intense as continental convection with respect to the updraft strength (contradicting the assumption of the G_updr lightning parameterisation), since the parameterisations provides only grid box mean updraft mass fluxes. The convective precipitation over the tropical oceans is too high (see Tost et al., 2006), leading to an overestimation of the flash frequencies from the A_prec parameterisation over the ocean.

- The annual cycle of convective events in the central tropics, i.e. the meridional movement of the strongest convection (the ITCZ) across the equator twice a year, is not reproduced well by any of the convection schemes. It is unclear whether this is a weakness of the convection parameterisations or of the model physics in general.

- Even though the influence of subgrid-scale convection on the humidity and moist static energy is captured accurately by the parameterisation independent of the model resolution, the convective dynamics can differ substantially, influencing both lightning schemes and convective tracer transport.

5 Conclusions

Using parameterised model results (convection) as input data for another parameterisation (lightning) leads to large uncertainties in the prediction of flashes and lightning produced NO_x emissions. For all combinations of lightning and convection schemes a scaling factor (in addition to the anyway performed resolution dependent rescaling) must be applied to reproduce the observed global flash frequency, and these factors can differ by orders of magnitude. With none of the combinations it is possible to accurately reproduce the observed lightning distributions, although some combinations are more suitable than others. The P_cth approach offers robustness with respect to both spatial and temporal variations of the convective events, but it is not very "physical", since cloud top height is not directly related to cloud electrification. The updraft approaches must be used very carefully, especially the G_updr scheme, since the exponential formulation tends to create unrealistically high values with strong updrafts. However, in combination with T1 this approach is among the best in reproducing the observed lightning densities. This results mainly from the development of the G_updr scheme in combination with this specific convection scheme in a previous model version (ECHAM4) (Grewe et al., 2001; Kurz and Grewe, 2002). The precipitation approach has shown to perform acceptably for the long-term average if the observed precipitation distribution is reproduced (e.g. by B1), whereas the temporal variability is hardly captured. Especially since the correlation between observed monthly mean precipitation and lightning is low, the performance is mainly a result of the fitting function. The annual cycle is difficult to reproduce with all combinations, indicating general problems with the models or parameterisation concepts. Even if the lightning events agree with the observations, the resulting NO_x emissions deviate due to the different convective cloud properties (freezing level, distinction between cloud-to-ground and intra-cloud flashes, etc.). From these results it is not possible to decide which emission profiles are most realistic since direct emissions are not observed. Only the combination of lightning emissions with a chemistry model can be evaluated using aircraft

observations in the anvil regions of convective clouds, which will be the focus of an upcoming study. The large variability associated with the tested combinations points to many unresolved problems in simulating lightning and lightning produced NO_x emissions in atmospheric general circulation models. Some approaches, e.g. the high correlation between precipitation ice and flash frequencies (Petersen et al., 2005) are promising, though require both improvements of the convection parameterisations with respect to ice microphysics and the development of a scheme that makes use of this relationship.

Appendix A

Abbreviations

σ	standard deviation
σ_{sim}	standard deviation of the simulation results
σ_{obs}	standard deviation of the observations
σ^*	$\sigma_{sim}/\sigma_{obs}$
R	correlation
GCM	General Circulation Model
AC-GCM	Atmospheric Chemistry General Circulation Model
ECMWF	European Centre for Medium Range Weather Forecast
E5/M1	ECHAM5/MESSy1
MATCH	Model of Atmospheric Transport and Chemistry
LNOX	NO_x emissions from lightning
TRMM	Tropical Rainfall Measuring Mission
ITCZ	Inner Tropical Convergence Zone
SPCZ	Southern Pacific Convergence Zone
LIS	Lightning Imaging Sensor
OTD	Optical Transient Detector
LISOTD_LRTS_V2.2	Low resolution time series dataset of combined flash rates from LIS and OTD
LISOTD_LRADC_V2.2	Low resolution annual diurnal climatology dataset of combined flash rates from LIS and OTD
T1	Tiedkte-Nordeng convection scheme
EC	convection scheme from ECMWF
ZH	convection scheme of Zhang-McFarlane-Hack
ZHW	convection scheme of Zhang-McFarlane-Hack with additional evaporation following Wilcox
B1	convection scheme of Bechtold
P_cth	lightning parameterisation based on cloud top height (Price and Rind)
G_updr	lightning parameterisation based on vertical velocity (Grewe)
A_updr	lightning parameterisation based on vertical velocity (Allen and Pickering)
G_updr	lightning parameterisation based on convective surface precipitation (Allen and Pickering)

Acknowledgements. We acknowledge the work of H. Christian and co-workers, providing the detailed lightning satellite observation data. We are further grateful to the TRMM satellite data team for providing their datasets. We thank V. Grewe and C. Kurz for their helpful comments to this manuscript and their contributions to the LNOX submodel development, and all the other MESSy developers for their support. Furthermore, we wish to acknowledge use of the Ferret program for analysis and graphics in this paper. Ferret is a product of NOAA's Pacific Marine Environmental Laboratory. (Information is available at http://ferret.pmel.noaa.gov/Ferret/). This study is part of the ENIGMA project; the authors thank the Max-Planck Society for support.

References

Allen, D. J. and Pickering, K. E.: Evaluation of lightning flash rate parameterizations for use in a global chemical transport model, J. Geophys. Res., 107, 4711, doi:10.1029/2002JD002066, 2002. 6772, 6777

Barthe, C., Molinié, G., and Pinty, J.-P.: Description and first results of an explicit electrical scheme in a 3D cloud resolving model, Atmos. Res., 76, 95–113, 2005. 6768

Bechtold, P., Bazile, E., Guichard, F., Mascart, P., and Richard, E.: A mass-flux convection scheme for regional and global models, Q. J. R. Meteorol. Soc., 127, 869–886, 2001. 6771

Bechtold, P., Chaboureau, J.-P., Beljaars, A., Betts, A. K., Köhler, M., Miller, M., and Redelsperger, J.-L.: The simulation of the diurnal cycle of convective precipitation over land in a global model, Quart. J. Roy. Meteorol. Soc., 130, 3119–3137, 2004. 6771

Beirle, S., Platt, U., Wenig, M., and Wagner, T.: NO_x production by lightning estimated with GOME, Adv. Space Res., 34, 793–797, 2004. 6769

Christian, H. J., Blakeslee, R. J., Goodman, S. J., Mach, D. A., Stewart, M. F., Buechler, D. E., Koshak, W. J., Hall, J. M., Boek, W. L., Driscoll, K. T., and Boccippio, D. J.: The Lightning Imaging Sensor, in: Proceedings of the 11th International Conference on Atmospheric Electricity, Guntersville, Alabama, 7–11 June, pp. 746–749, 1999. 6769, 6774

Christian, H. J., Blakeslee, R. J., Boccippio, D. J., Boeck, W. L., Buechler, D. E., Driscoll, K. T., Goodman, S. J., Hall, J. M., Koshak, W. J., Mach, D. M., and Stewart, M. F.: Global frequency and distribution of lightning as observed from space by the Optical Transient Detector, J. Geophys. Res., 108, 4005, doi:10.1029/2002JD002347, 2003. 6769, 6774

Grewe, V., Brunner, D., Dameris, M., Grenfell, J. L., Hein, R., Shindell, D., and Staehelin,

J.: Origin and variability of upper tropospheric nitrogen oxides and ozone at northern mid-latitudes, Atmos. Environ., 35, 3421–3433, 2001. 6772, 6775, 6787

Hack, J. J.: Parameterization of moist convection in the National Center for Atmospheric Research community climate model (CCM2), J. Geophys. Res., 99, 5551–5568, 1994. 6771, 6776

Jacobson, M. Z.: Atmopsheric Pollution, Cambridge University Press, 2002. 6768

Jeuken, A. B. M., Siegmund, P. C., Heijboer, L. C., Feichter, J., and Bengtsson, L.: On the potential of assimilating meteorological analyses in a global climate model for the purpose of model validation, J. Geophys. Res., 101, 16 939–16 950, 1996. 6773

Jöckel, P., Sander, R., Kerkweg, A., Tost, H., and Lelieveld, J.: Technical Note: The Modular Earth Submodel System (MESSy) – a new approach towards Earth System Modeling, Atmos. Chem. Phys., 5, 433–444, 2005, http://www.atmos-chem-phys.net/5/433/2005/. 6770

Jöckel, P., Tost, H., Pozzer, A., Brühl, C., Buchholz, J., Ganzeveld, L., Hoor, P., Kerkweg, A., Lawrence, M. G., Sander, R., Steil, B., Stiller, G., Tanarhte, M., Taraborrelli, D., van Aardenne, J., and Lelieveld, J.: The atmospheric chemistry general circulation model ECHAM5/MESSy1: consistent simulation of ozone from the surface to the mesosphere, Atmos. Chem. Phys., 6, 5067–5104, 2006, http://www.atmos-chem-phys.net/6/5067/2006/. 6770, 6773

Kummerow, C., Simpson, J., Thiele, O., Barnes, W., Chang, A. T. C., Stocker, E., Adler, R. F., Hou, A., Kakar, R., Wentz, F., Ashcroft, P., Kozu, T., Hong, Y., Okamoto, K., Iguchi, T., Kuroiwa, H., Im, E., Haddad, Z., Huffman, G., Ferrier, B., Olson, W. S., Zipser, E., Smith, E. A., Wilheit, T. T., North, G., Krishnamurti, T., and Nakamura, K.: The Status of the Tropical Rainfall Measuring Mission (TRMM) after two years in orbit, J. Appl. Meteorol., 39, 1965–1982, 2000. 6774

Kurz, C. and Grewe, V.: Lightning and thunderstorms, Part I: Observational data and model results, Met. Zeitschr., 11, 379–393, doi:10.1127/0941-2498/2002/0011-0379, 2002. 6785, 6787

Labrador, L. J., v. Kuhlmann, R., and Lawrence, M. G.: The effects of lightning-produced NO_x and its vertical distribution on atmospheric chemistry: sensitivity simulations with MATCH-MPIC, Atmos. Chem. Phys., 5, 1815–1834, 2005, http://www.atmos-chem-phys.net/5/1815/2005/. 6768

Lawrence, M. G., Crutzen, P. J., Rasch, P. J., Eaton, B. E., and Mahowald, N. M.: A model for studies of tropospheric chemistry: Description, global distributions and evaluation, J.

Geophys. Res., 104, 26 245–26 277, 1999. 6771

Nickolaenko, A. P., Hayakawa, M., and Sekiguchi, M.: Variations in global thunderstorm activity inferred from the OTD records, Geophys. Res. Lett., 33, L06 823, doi:10.1029/2005GL024884, 2006. 6782

Nordeng, T. E.: Extended versions of the convective parametrization scheme at ECMWF and their impact on the mean and transient activity of the model in the tropics, Tech. Rep. 206, ECWMF, 1994. 6771

Petersen, W. A. and Rutledge, S. A.: On the relationship between cloud-to-ground lightning and convective rainfall, J. Geophys. Res., 103, 14 025–14 040, 1998. 6769, 6770, 6780

Petersen, W. A., Christian, H. J., and Rutledge, S. A.: TRMM observations of the global relationship between ice water content and lightning, Geophys. Res. Lett., 32, L14 819, doi:10.1029/2005GL023236, 2005. 6770, 6788

Pickering, K. E., Wang, Y., Tao, W.-K., Price, C., and Müller, J.-F.: Vertical distribution of lightning NO_x for use in regional and chemical transport models, J. Geophys. Res., 103, 31 203–31 216, 1998. 6773

Price, C. and Rind, D.: A simple Lightning Parametrization for Calculating Global Lightning Distributions, J. Geophys. Res., 97, 9919–9933, 1992. 6771

Price, C. and Rind, D.: What determines the Cloud-to-Ground Lightning fraction in Thunderstorms, Geophys. Res. Lett., 20, 463–466, 1993. 6771, 6773

Price, C. and Rind, D.: Modeling Global Lightning Distributions in a General Circulation Model, Mon. Wea. Rev., 122, 1930–1939, 1994. 6772, 6782

Price, C., Penner, J., and Prather, M.: NO_x from lightning, 1. Global distribution based on lightning physics, J. Geophys. Res., 102, 5929–5941, 1997a. 6772

Price, C., Penner, J., and Prather, M.: NO_x from lightning, 2. Constraints from the global atmospheric electric circuit, J. Geophys. Res., 102, 5943–5951, 1997b. 6772

Rasch, P. J., Mahowald, N. M., and Eaton, B. E.: Representations of transport, convection and the hydrologic cycle in chemical transport models: Implications for the modeling of short-lived and soluble species, J. Geophys. Res., 102, 28 127–28 138, 1997. 6771

Roeckner, E., Bäuml, G., Bonaventura, L., Brokopf, R., Esch, M., Giorgetta, M., Hagemann, S., Kirchner, I., Kornblue, L., Manzini, E., Rhodin, A., Schleese, U., Schulzweida, U., and Tompkins, A.: The atmospheric general circulation model ECHAM5: Part 1, Tech. Rep. 349, Max-Planck-Institut für Meteorologie, 2003. 6771

Roeckner, E., Brokopf, R., Esch, M., Giorgetta, M., Hagemann, S., Kornblue, L., Manzini, E.,

Schleese, U., and Schulzweida, U.: The atmospheric general circulation model ECHAM5: Part 2, Tech. Rep. 354, Max-Planck-Institut für Meteorologie, 2004. 6771

Roeckner, E., Brokopf, R., Esch, M., Giogetta, M., Hagemann, S., Kornblueh, L., Manzini, E., Schleese, U., and Schulzweida, U.: Sensitivity of simulated climate to horizontal and vertical resolution in the ECHAM5 atmosphere model, J. Clim., 19, 3771–3791, 2006. 6770

Schumann, U. and Huntrieser, H.: The global lightning-induced nitrogen oxides source, Atmos. Chem. Phys. Discuss., 7, 2623–2818, 2007, http://www.atmos-chem-phys-discuss.net/7/2623/2007/. 6768, 6769

Taylor, K. E.: Summarizing multiple aspects of model preformance in a single diagram, J. Geophys. Res., 106, 7183–7192, 2001. 6778

Thomas, R. J., Krehbiel, P. R., Rison, W., Hamlin, T., Boccippio, D. J., Goodman, S. J., and Christian, H. J.: Comparison of ground-based 3-dimensional lightning mapping observations with satellite-based LIS observations in Oklahoma, Geophys. Res. Lett., 27, 1703–1706, 2000. 6769, 6774

Tiedtke, M.: A Comprehensive Mass Flux Scheme for Cumulus Parametrization in Large-Scale Models, Mon. Wea. Rev., 117, 1779–1800, 1989. 6771, 6786

Tost, H.: Global Modelling of Cloud, Convection and Precipitation Influences on Trace Gases and Aerosols, Ph.D. thesis, Rheinische Friedrich-Wilhelms-Universität Bonn, Germany, available at: http://hss.ulb.uni-bonn.de/diss_online/math_nat_fak/2006/tost_holger, 2006. 6771, 6777, 6786

Tost, H., Jöckel, P., and Lelieveld, J.: Influence of different convection parameterisations in a GCM, Atmos. Chem. Phys., 6, 5475–5493, 2006, http://www.atmos-chem-phys.net/6/5475/2006/. 6770, 6771, 6777, 6778, 6786

van Aalst, M. K., van den Broek, M. M. P., Bregman, A., Brühl, C., Steil, B., Toon, G. C., Garcelon, S., Hansford, G. M., Jones, R. L., Gardiner, T. D., Roelofs, G.-J., Lelieveld, J., and Crutzen, P.: Trace gas transport in the 1999/2000 Arctic winter: comparison of nudged GCM runs with observations, Atmos. Chem. Phys., 4, 81–93, 2004, http://www.atmos-chem-phys.net/4/81/2004/. 6773

Wilcox, E. M.: Spatial and Temporal Scales of Precipitation Tropical Cloud Systems in Satellite Imagery and the NCAR CCM3, J. Climate, 16, 3545–3559, 2003. 6771

Zhang, G. J. and McFarlane, N. A.: Sensitivity of Climate Simulations to the Parameterization of Cumulus Convection in the Canadian Climate Centre General Circulation Model, Atmosphere-Ocean, 33, 407–446, 1995. 6771, 6776

Table 1. Scaling factors for the combination of lightning and convection parameterisations.

	P_cth	G_updr	A_updr	A_prec
T1	5.92	4.28	4.22	2.78
EC	2.14	1.37	5.26	5.52
ZH	0.87	434.73	148.18	24.27
ZHW	0.74	227.32	114.95	18.69
B1	1.36	1.35	20.74	3.97

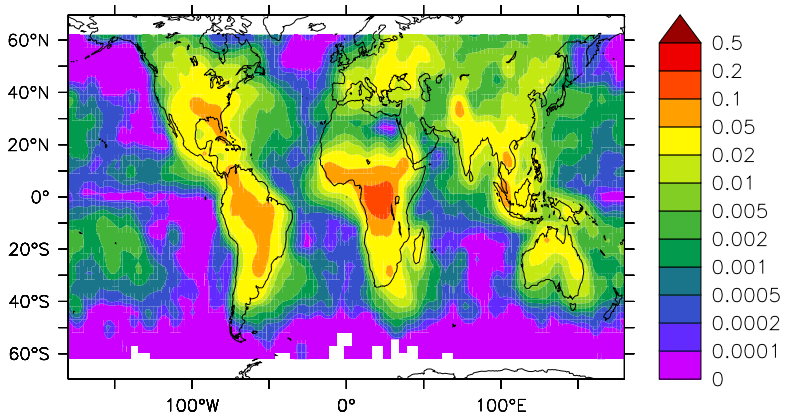

Fig. 1. Observed annual average flash density in flashes/(km^2 day) for the year 1999 from LIS/OTD data from 60° S to 60° N.

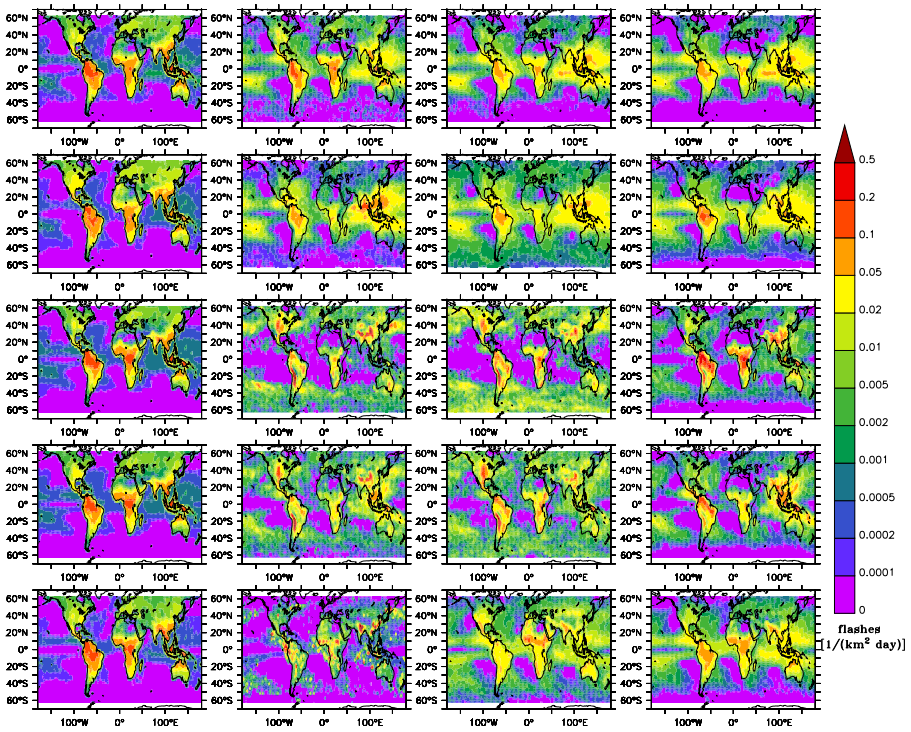

Fig. 2. Annual average global lightning distribution from 60° S to 60° N in flashes/(km^2 day). The rows represent the different convection schemes (T1, EC, ZH, ZHW, B1 from top to bottom), whereas the columns depict the different lightning parameterisations (P_cth, G_updr, A_updr, A_prec from left to right).

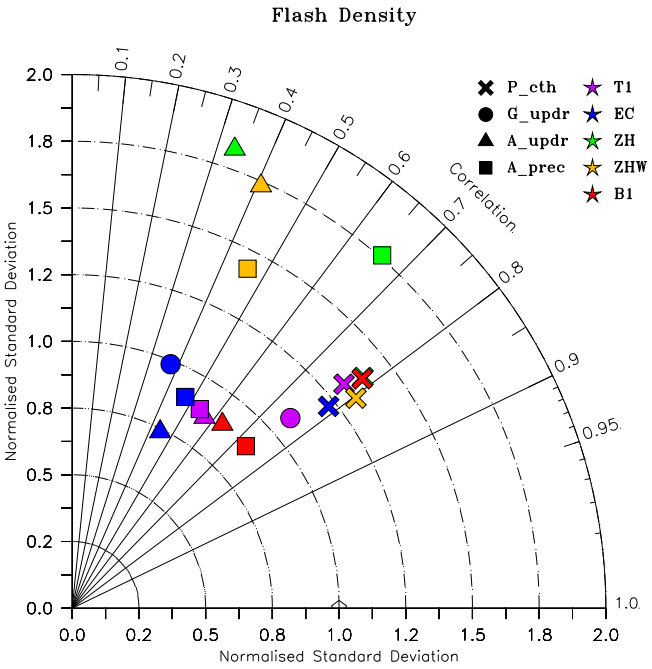

Fig. 3. Taylor diagram for the various combinations of convection and lightning schemes compared with LIS/OTD data, showing the standard deviation of the calculated flash densities normalised with the standard deviation of the observations σ^* (on the radial axis), the correlation R (the angle) and the RMSE (distance from the point marked with a open box with correlation of one and normalised standard deviation of one). The different convection schemes are depicted by the colours, and the lightning parameterisations by the symbols.

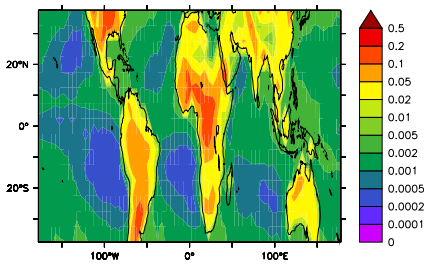

Fig. 4. Parameterised annual average flash density (in flashes/(km^2 day)) from TRMM monthly mean cloud top height for the year 1999, applying the P_cth scheme. The lightning activity has been rescaled to the observations as described above.

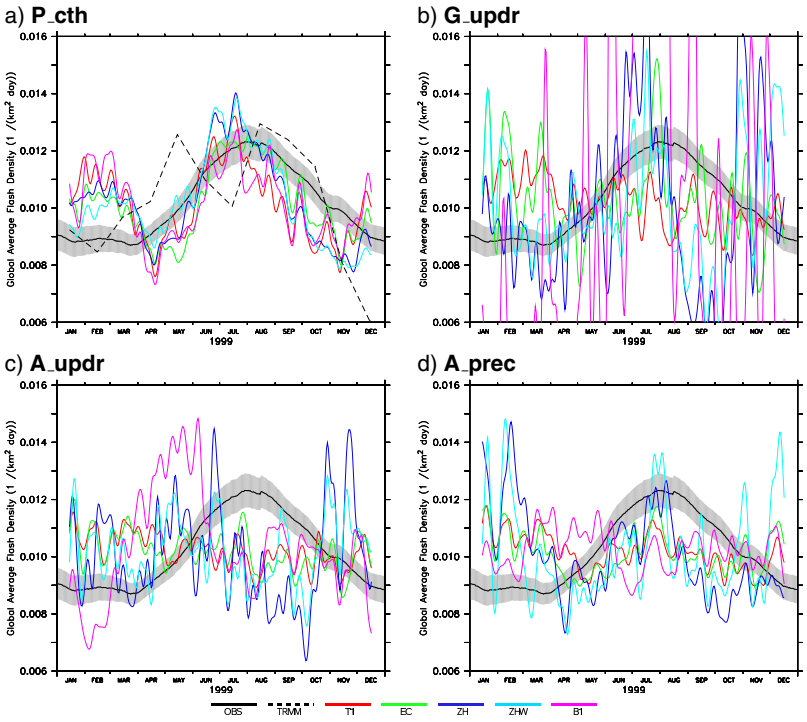

Fig. 5. Average (60° S to 60° N, for the TRMM data only 40° S to 40° N) time series of the flash density for the year 1999. The four panels show the different lightning schemes. The black line depicts the observations and the grey shaded area the spatial standard deviation. The coloured lines represent the model simulations with the different convection schemes.

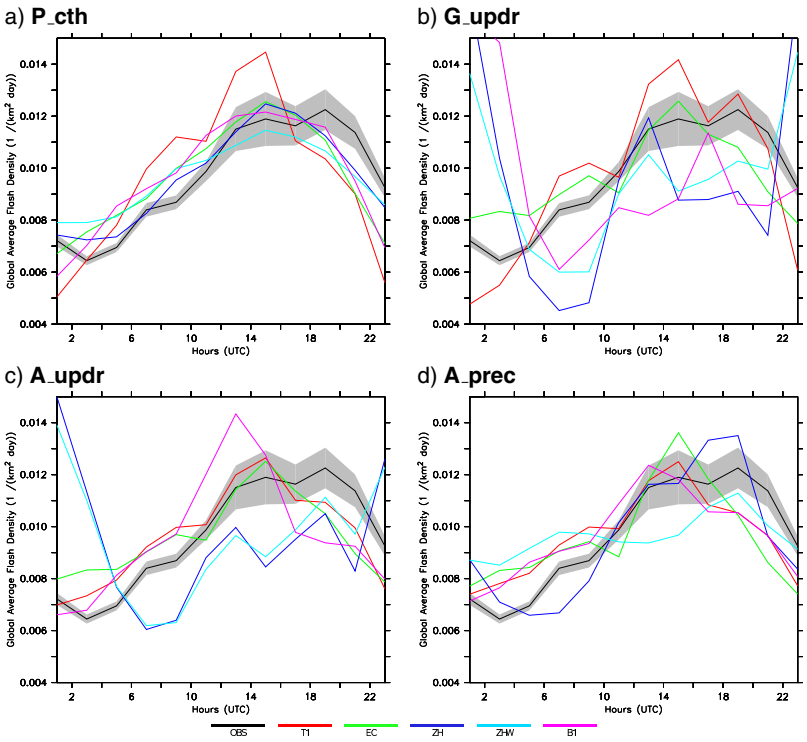

Fig. 6. Global average diurnal time series of the flash density for the year 1999. The four panels show the different lightning schemes. The black line depicts the observations (multi-year climatology) and the grey shaded area the spatial standard deviation (one σ). The coloured lines represent the model simulations with the different convection schemes.

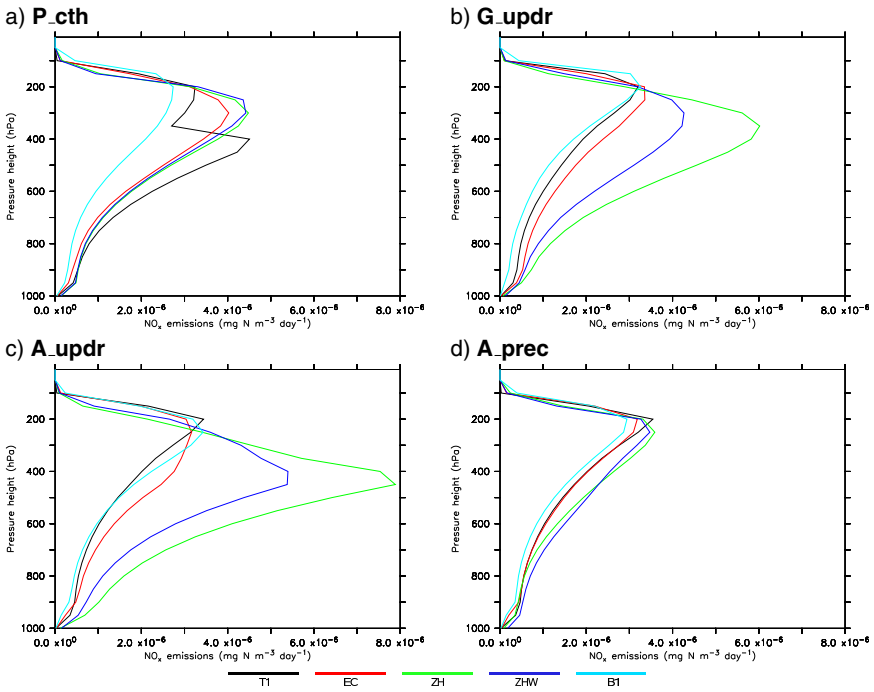

Fig. 7. Vertical profiles of the annual average lightning produced NO_x emissions, spatially averaged (meridional and zonal, the latter restricted to 60° S–60° N). As in Fig. 5 the panels display the lightning schemes, and the colours the convection parameterisations.